Proceedings of the Canadian Society for Mechanical Engineering International Congress
32nd Annual Conference of the Computational Fluid Dynamics Society of Canada
Canadian Society of Rheology Symposium
CSME-CFDSC-CSR 2025
May 25–28, 2025, Montréal, Québec, Canada

ESTIMATION OF ARC EFFICIENCY IN ARC WELDING USING TEMPERATURE MEASUREMENTS

G. J. A. de Andrade[1], D. Groulx[1*], W. B. da Silva[2]
[1]Department of Mechanical Engineering, Dalhousie University, Halifax, Canada
[2]Department of Rural Engineering, Federal University of Espirito Santo, Alegre, Brazil
*e-mail address: dominic.groulx@dal.ca

Abstract— This research investigates the use of the Sample Importance Resampling (SIR) filter to estimate the efficiency of an arc used in welding or additive manufacturing (AM) in order to determine if the method is capable of such estimation. It is known that the amount of energy delivered to parts during welding affects their microstructures and mechanical properties; therefore, an accurate knowledge of the heat input is of paramount importance. Researchers have been utilizing multiple approaches to assess the energy inputs including calorimetry and Inverse Heat Transfer Problems (IHTP). In this study a three-dimensional transient analytical solution that incorporates a double ellipsoidal heat source was considered. Results show that SIR was able to estimate the thermal efficiency of the arc during welding for different scenarios.

Keywords – Arc Efficiency; Arc Welding; Gas Metal Arc Welding (GMAW); Sample Importance Resampling (SIR); Inverse Heat Transfer Problems (IHTP).

I. INTRODUCTION

Thermal field variations caused by the heat input of a welding torch strongly influence the mechanical properties of materials. During welding, a portion of the power from the welding torch is lost to the environment by convection and radiation while the rest enters the part. The ratio between the heat that is actually admitted by the part (Q_{in}) and the nominal power input from the power supply (Q_{non}) is defined as the arc efficiency (η_{arc}). Therefore, it is crucial to know the arc efficiency for a proper representation of the welding process in a numerical simulation [1].

The estimation of the arc efficiency is commonly reported to be made by means of the Seebeck calorimeter, in which the working fluid to cool down the samples is water [1, 2]. Despite the method being reported to achieve an accuracy of within 1%, there is the inconvenience that, once the sample is placed in the calorimeter, each measurement can take as long as 6 hours [3]. The use of liquid nitrogen in calorimeters is also reported in the literature, having the advantage of being faster [1]. Likewise, heat losses are observed in calorimeter techniques before the sample being placed inside the calorimeter [1] and subjected to heat losses during the welding [4]. The economic cost of calorimetric methods is another drawback [5].

The use of the Inverse Heat Transfer Problem (IHTP) is an alternative to prevent the disadvantages of calorimetric methods [5]. Inverse problems can be broadly defined as those dealing with the estimation of unknown quantities appearing in the mathematical formulation of any kind of process, by using measurements of some of the problem's observable response [6, 7]. Gonçalves *et al.* [8] used Simulated Annealing and the Golden Section method in an optimization approach of IHTP considering two heat transfer models to estimate the arc efficiency in an arc welding process. Magalhães *et al.* [5] used the Golden Section method and Time Traveling Regularization to estimate the heat input in an arc welding process. Nonetheless, since the optimization approach of IHTP usually seeks to minimize an objective function, it may lead to local minimum. Also, these methods neglect the statistical nature of the uncertainties present in a measurement system [9].

On the other hand, within the Bayesian approach of IHTP, the transient problems are treated as state estimation problems, in which the available measurement data is combined with prior knowledge of the underlying physical phenomena (as described by the direct problem) and measurement systems to sequentially estimate the evolving dynamic variables of interest. Particle Filters have been developed as a robust alternative in Bayesian Approach of IHTP [3]. Amongst particle filters, the Sample Importance Resampling (SIR) filter has the advantage of preventing the degeneracy problem observed in other particle filter methods, in which large computational efforts are devoted to update particles with low contributions. This advantage is due to the resampling step of the SIR filter, in which particles with low weights are eliminated and the ones with high weights are replicated [3]. Therefore, the objective of this research is to determine if the SIR filter is capable of estimating the arc efficiency in an arc welding process.

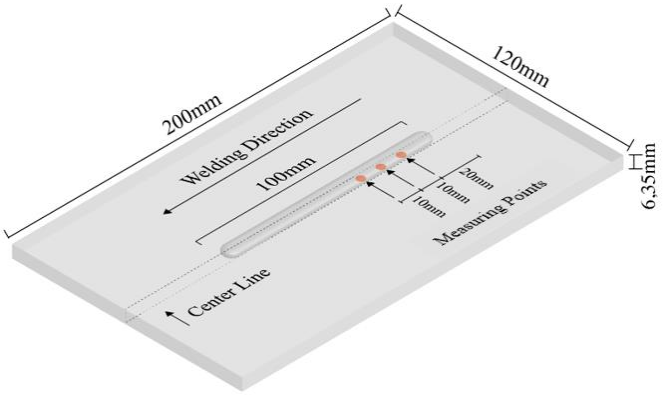

Figure 1. Schematic representation of system considered in this research with the welding bead, welding plate, and three points where measurements are taken.

II. Mathematical Problem

The physical problem considered in this research involves heat conduction through a plate, as presented in Fig. 1, caused by heat input during an arc welding process. Fachinotti *et al.* [10] presented a solution for the three-dimensional transient heat conduction problem considering a double ellipsoidal moving heat source with thermal properties constant with temperature, in a semi infinity homogeneous solid medium, of which the solution is presented in Eq. (1).

$$T(x,y,z,t) = T_0 + \frac{3\sqrt{3}Q_{non}\eta_{arc}}{\pi\sqrt{\pi}\rho c_p} \times \int_0^t \exp\left[\frac{-3\frac{y^2}{12\alpha(t-t')+a^2}-3\frac{z^2}{12\alpha(t-t')+b^2}}{\sqrt{12\alpha(t-t')+a^2}\sqrt{12\alpha(t-t')+b^2}}\right] \times \left[f_r A_r(1-B_r) + f_f A_f\left(1+B_f\right)\right] dt' \quad (1)$$

where $T(x,y,z,t)$ is the transient temperature field, T_0 is the initial temperature of the plate under welding, Q_{non} is the power that leaves the welding torch, η_{arc} is the arc efficiency, c_p is the specific heat of the plate, v is the velocity of the heat source and α is the thermal diffusivity. A and B are written for convenience, they do not have any physical meaning and are given by Eqs. (2) and (3):

$$A_i = A(x,t,t';c_i) = \frac{\exp\left[\frac{-3(x-vt')^2}{12\alpha(t-t')+c_i^2}\right]}{\sqrt{12\alpha(t-t')+c_i^2}} \quad (2)$$

$$B_i = B(x,t,t';c_i) = \operatorname{erf}\left[\frac{c_i}{2}\frac{x-vt'}{\sqrt{\alpha(t-t')}\sqrt{12\alpha(t-t')+c_i^2}}\right] \quad (3)$$

where parameters of the double ellipsoidal heat source, also known as the Goldak heat source [11], are a the distance from the focus to the inferior limit in the z direction and b the distance from the focus to limit in the y direction. Also, c_f and c_r are the respective distances from focus to front and rear in the xy plane,

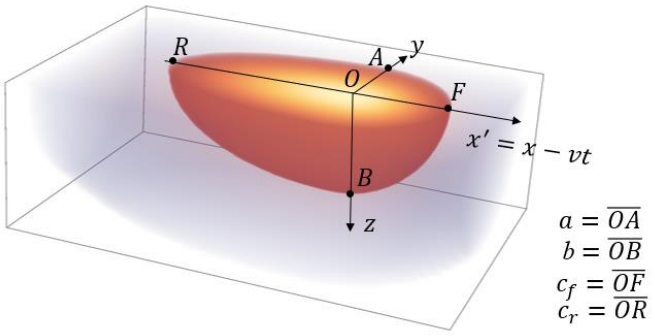

Figure 2. Representation of the Goldak heat source with the defined geometric parameters.

TABLE I. PARAMETERS OF THE GOLDAK HEAT SOURCE

a(m)	b (m)	c_r(m)	c_f(m)	f_f(m)	f_f(m)
0.003935	0.0026	0.00197	0.00787	0.6	1.4

TABLE II. THERMAL PROPERTIES OF ASTM-A36 AT 25 °C

ρ (kg/m³)	k (W/m.K)	c_p (J/kg.K)
7832.05	51.41401	454.82

as shown in Fig. 2. In addition, f_r and f_f are the portion of the heat deposited, respectively, in the rear and front of the ellipsoid (with $f_r + f_f = 2$). The index i assumes r for the rear or f for the front, depending on the portion of the heat source.

The values of these parameters adopted in this research were obtained by following the recommendations of Goldak *et al.* [11] and are presented in Table I. The time integral in Eq. (1) can only be solved numerically; for this work, this integral was calculated using the function quad from the sub-package *SciPy.Integrate* of the *SciPy* package for *Python*.

The process parameters utilized in this research are from Arruda *et al.* [12]. The power delivered is Q_{non} = 3642.4 W, and the velocity of the moving heat source is v = 0.00535 m/s. The plate material is ASTM – A36 steel. The thermal properties at 25 °C are presented in Table II.

III. Inverse Problem

The particle filter method utilizes the posterior density represented by a set of particles with associated weights. Consider the following state evolution model for the vector of state variables **x:**

$$\mathbf{x}_k = \mathbf{f}_k(\mathbf{x}_{k-1}, v_k) \quad (4)$$

where the subscript $k = 1,2 \ldots$, is the timestep t_k in a dynamic problem and **f** is a non-linear function of the state variables **x,** v is the state noise vector. In addition, the relation between the measures **z** and the state variables **x** through a general function **h**, in the observation (measurement) model, given by Eq. (5).

$$\mathbf{z}_k = \mathbf{h}_k(\mathbf{x}_k, n_k) \quad (5)$$

where n represents uncertainty associated with the measurements. The state estimation problem seeks to gather information about $\mathbf{x}_k$ using the state evolution model and the measurement of $\mathbf{z}_{1:k}^i = \{z_i, 1, \dots, k\}$ [13]. Therefore, considering $\{x_{0:k}^i, i = 0, \dots, N_{part}\}$ as the particles associated with the weights, $\{w_{1:k}, i = 0, \dots, N_{part}\}$ and $\mathbf{x}_{0:k} = \{\mathbf{x}_j, j = 0, \dots, k\}$ as the set of all state variables up to the timestep k, where N_{part} is the number of particles. Then, the marginal distribution of $\mathbf{x}_k$, which is the interest for the filtering problem, can be approximated by the Eq. (6) [7, 14]:

$$\pi(x_k \mid z_{1:k}) \approx \sum_{i=1}^{N} w_k^i \delta(x_k - x_k^i) \tag{6}$$

where δ is the Dirac delta distribution. The SIR filter algorithm is summarized as in Table III [14]. In this research $\mathbf{x}_k = (\mathbf{T}_{est}^k, \eta_{arc}^k)$, where $\mathbf{T}_{est}^k$ is the vector of temperature estimation at the three measuring points.

The state evolution model of temperatures in space is given by Eq. (1). The uncertainties for this model were considered additive, Gaussian with zero mean and standard deviation of 1% of temperature value. Since the evolution of η_{arc} is not a priori known, a random walk model was adopted:

$$\eta_{arc}^{k+1} = \eta_{arc}^k + \sigma_\eta \times U(-1,1) \tag{7}$$

where $\eta_{arc}^k = \eta_{arc}(t)$ is the arc efficiency at each timestep, $U(-1,1)$ is a random number with uniform distribution from -1 to 1, and σ_η is the standard deviation of the random walk.

It is known from the theory of arc welding that the arc efficiency in Gas Metal Arc Welding (GMAW) varies from 65% to 90% of nominal power. Therefore, the random walk was limited to values from 75% to 85% [15].

TABLE III. SIR FILTER ALGORITHM

Step 1. For $i = 1, \dots, N_{part}$, draw new particles x_k from the prior density $\pi(\mathbf{x}_k \mid \mathbf{x}_{k-1}^i)$ and then use the likelihood function to calculate the corresponding weights $w_k^i = \pi(\mathbf{z}_k \mid \mathbf{x}_k^i)$.
Step 2. Calculate the total weight $Total_w = \sum_{i=1}^{N} w_k^i$ and then normalize the particle weights, i.e. for $i = 1,\dots,N_{part}$ let $w_k^i \leftarrow w_k^i / Total_w$
Step 3. Resample the particles as follows: Construct the cumulative sum of weights (CSW) by computing $c_i = c_{i-1} + w_k^i$ for $i = 1, \dots, N_{part}$ starting from $c_0 = 0$. Let $i = 1$ and draw a starting point u_1 from the uniform distribution $U[0, N_{part}{}^{-1}]$. For $j = 1, \dots, N_{part}$: Move along the CSW by defining $u_j = u_1 + (j-1)/N_{part}$. While $u_j > c_i$ do $i = i + 1$. Assign sample $\mathbf{x}_k^{(j)} \leftarrow \mathbf{x}_k^{(i)}$. Assign sample weight $w_k^j = 1/N_{part}$.

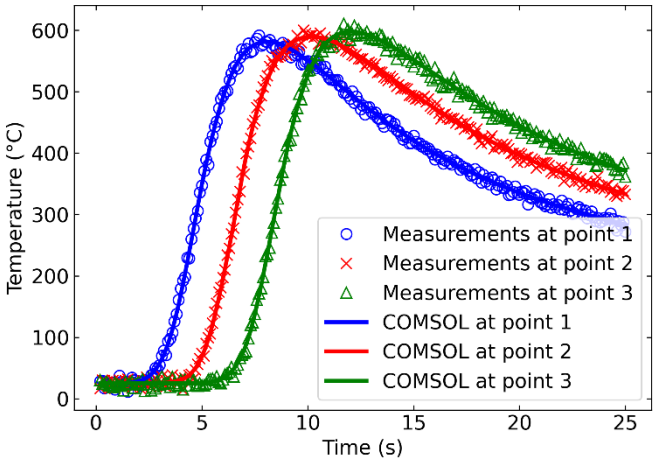

Figure 3. Simulated measurements of temperature at three different points.

Due to the limitations of the model presented in Eq. (1) multiple simulations of SIR filter were performed to obtain an uncertainty of the model that would compensate for the limitations of the analytical solution.

IV. RESULTS AND DISCUSSION

The estimation of η_{arc}^k with the SIR algorithm was examined by using simulated temperature measurements of sensors located at the opposite surface along the central line of the plate at x_1= 0.02 m, x_2= 0.03 m and x_3= 0.04 m, as Fig. 1 depicts. For each second, in a process of 25 seconds, 10 measurements of temperature were taken, these measurements are presented in Fig. 3. The simulation of temperature measurements was obtained with COMSOL Multiphysics considering η_{arc}= 80%. Equation (8) was applied to perturb the numerical results.

$$T_{meas}^k = T_{numerical}^k + \delta^k \tag{8}$$

$$\delta^k = 1\% \times Max(T_{Numerical}) \times N(0,1) \tag{9}$$

where T_{meas} are the simulated measurements of temperature, $T_{Numerical}$ is the temperature from the numerical simulation in COMSOL, δ_{error} is an additive gaussian noise that represents the measuring error, and $N(0,1)$ is a random number with zero as mean and standard deviation as one.

The numerical solution was determined with COMSOL Multiphysics considering thermal properties as functions of temperature, these properties were obtained by means of JMatPro for ASTM-A36 Stell. The state evolution model is given by the Eq. (10).

$$\begin{aligned} T_{est}^k &= T_{est}^{k-1} \\ &+ \frac{3\sqrt{3}Q_{non}\eta_{arc}^k}{\pi\sqrt{\pi}\rho c_p}\left(\int_0^t \Phi(x,y,z,t,t')\,dt' \right. \\ &\left. - \int_0^{t_{k-1}} \Phi(x,y,z,t,t')\,dt'\right)\sigma_T N(0,1) \end{aligned} \tag{10}$$

where $\Phi(x,y,z,t,t')$ is written for convenience and given by Eq. (11):

$$\Phi(x,y,z,t,t') = exp\left[\frac{-3\frac{y^2}{12\alpha(t-t')+a^2}-3\frac{z^2}{12\alpha(t-t')+b^2}}{\sqrt{12\alpha(t-t')+a^2}\sqrt{12\alpha(t-t')+b^2}}\right]\left[f_r A_r(1-B_r)+ f_f A_f(1+B_f)\right] \quad (11)$$

where in Eq. (10) T_{est}^k is the estimated temperature at timestep k, σ_T is the uncertainty of the model, and $N(0,1)$ is a normal random number with zero mean and standard deviation one.

The simulation of SIR filter, took into account $\sigma_{\eta_{arc}} = 1\% \times \eta_{arc_0}$ and $\sigma_{\eta_{arc}} = 5\% \times \eta_{arc_0}$, where η_{arc_0}= 0.8, considering the following scenarios for σ_T, such as (a) $\sigma_T = 5\% \times Max(T_{Numerical})$, (b) $\sigma_T = 8\% \times Max(T_{Numerical})$, and (c) $\sigma_T = 10\% \times Max(T_{Numerical})$ to figure out the uncertainty of the model and the standard deviation of the random walk that would fit to the estimation considering the Root Mean Square Error (RMSE) presented in Eq. (12), Relative Error (Rel) in Eq. (13) where M is the number of measurements, k is the timestep, ρ_k is the expected value of the variable ρ, and $\hat{\rho}_k$ is the estimated value of that variable at timestep k.

$$\text{RMSE}_\rho = \sqrt{\frac{1}{M}\sum_{k=1}^{M}(\rho_k - \hat{\rho}_k)^2} \quad (12)$$

$$\text{Rel}(\rho) = \frac{\sqrt{\sum_{k=1}^{M}(\rho_k-\hat{\rho}_k)^2}}{\sqrt{\sum_{k=1}^{M}\rho_k^2}} \times 100\% \quad (13)$$

Additionally, the Number of Effective Samples (N_{eff_k}) is calculated by the Eq. (14), where N_{part} is the number of particles and w_k is the weight of the i^{th} particle of the SIR filter at the timestep k. Thus, a low N_{eff_k} indicates severe degeneration of the particle filter [16].

$$N_{eff_k} = \frac{1}{\sum_{i=1}^{N_{\text{part}}}\left(w_k^i\right)^2} \quad (14)$$

In this work, different number of particles were considered in order to determine the minimum needed that would be able to estimate η_{arc}. This was necessary since, for a real-time estimation, the time taken by the SIR filter must be equivalent to the time of welding.

The estimation of η_{arc} is presented in Figs. 4, 5, and 6 in terms of the arc efficiency mean values and their 95% credible interval (CI). The CI was calculated by the function *np.quantile* of the *NumPy* library for *Python* language. The exact values of η_{arc} are also shown with black lines.

In Fig. 4, the estimation of η_{arc} is observed considering $\sigma_T = 8\% \times Max(T_{Numerical})$ and $\sigma_{\eta_{arc}} = 5\% \times \eta_{arc_0}$ with 1000 particles, it is noticed that the estimated values of η_{arc} fluctuate around the exact value through the experiment and that these values tend to decrease. Moreover, it is observed that the CI through the experiment varies approximately from 0.75 to 0.85, which can be viewed as a large standard deviation. The estimation of η_{arc} and the exact value are within the 95% CI, indicating the η_{arc} estimation has 95 % probability of being within the CI along with the exact value. That was observed through the entire time of the experiment.

In Fig. 5 the estimation of the η_{arc} using 1000 particles, $\sigma_T = 5\% \times Max(T_{Numerical})$, and $\sigma_{\eta_{arc}} = 5\% \times \eta_{arc_0}$ is presented. The results are similar to those on of Fig. 4; however, in this case, the average of the η_{arc} estimations are slightly above the exact one during a major part of the experiment; but, similarly to the results of Fig. 4, the CI varies from 0.75 to 0.85 indicating a large standard deviation. The exact values of η_{arc} and the estimation are within the 95 % CI. Considering the wide CI, and its fluctuations, these estimations are considered good because the estimations of arc efficiency and the exact value are within the CI.

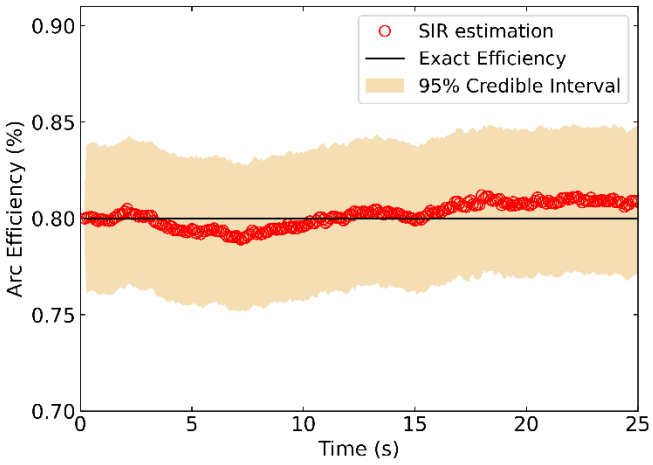

Figure 4. Estimation of the arc efficiency with 1000 particles $\sigma_T = 8\% \times Max(T_{Numerical})$, $\sigma_{\eta_{arc}} = 5\% \times \eta_{arc_0}$.

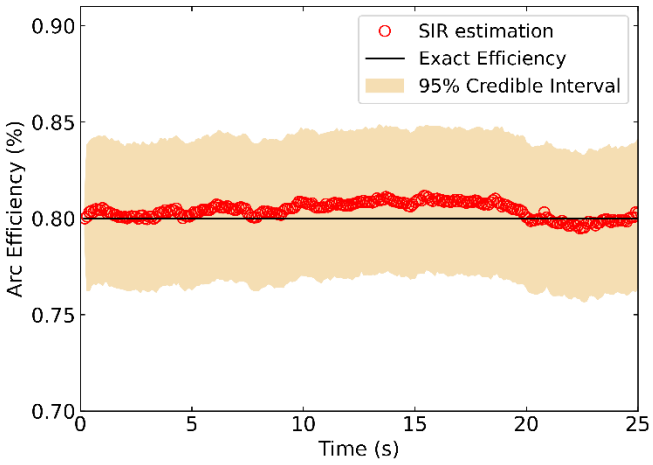

Figure 5. Estimation of the arc efficiency with 1000 particles $\sigma_T = 5\% \times Max(T_{Numerical})$ and $\sigma_{\eta_{arc}} = 5 \times \%\, \eta_{arc_0}$.

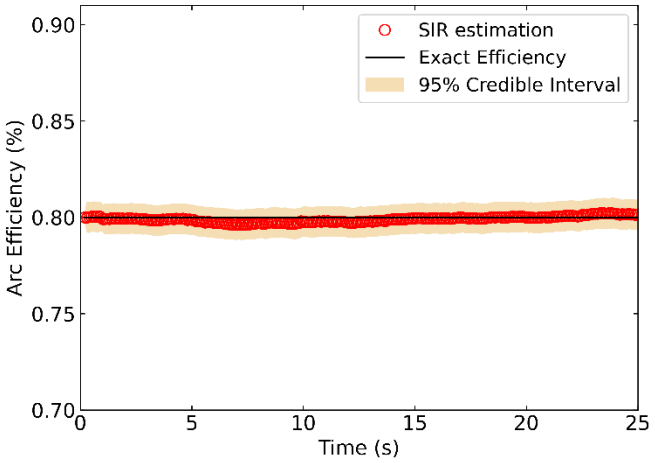

Figure 6. Estimation of the arc efficiency using 1000 particles $\sigma_T = 8\% \times Max(T_{Numerical})$, $\sigma_{\eta_{arc}} = 1\% \times \eta_{arc_0}$.

The problem with this wide CI, and its large standard deviation, is that the CI is approximately the same as the prior belief interval that was set to limit the random walk, that is, from 0.75 to 0.85, meaning that the SIR filter poorly improved the prior information about the arc efficiency, which can be interpreted as the standard deviation of the random walk was so high that the particles all over the interval from 0.75 to 0.85 were accepted by the algorithm, as a consequence a low accuracy estimation was obtained.

The accuracy of estimation was improved, as the minor width of CI suggests, by reducing the $\sigma_{\eta_{arc}}$, for instance, in Fig. 6 the estimation of η_{arc} with 1000 particles, $\sigma_T = 8\% \times Max(T_{Numerical})$ and $\sigma_{\eta_{arc}} = 1\% \times \eta_{arc_0}$ is presented. It is noticed that the algorithm was able to recover the exact value of arc efficiency within the CI. In addition, the narrow CI suggests a low standard deviation of the estimation. The curve of the estimated η_{arc} is practically identical to the exact one, the estimation of η_{arc} behaves even better than the previous ones, during the experiment.

The measurements of temperature are also estimated to validate the estimations of η_{arc} during a timestep k of the SIR filter algorithm. In Figs. 7, 8, and 9, the estimation of the measurements of temperatures, the simulated measurements of temperatures, and the temperatures obtained from COMSOL at $x_1 = 0.02$ m, $x_2 = 0.03$ m and $x_3 = 0.04$ m respectively are presented, considering, 1000 particles $\sigma_T = 8\% \times Max\,(T_{Numerical})$, and $\sigma_{\eta_{arc}} = 1\% \times \eta_{arc_0}$. The red squares are the means of temperature estimations, the blue circles are the simulated measurements of temperature, and the black line is the temperatures obtained from COMSOL. It is noticed that for the three measuring points, the temperatures from COMSOL are recovered with a good response to the changes of temperature, meaning that the estimations were able to track the variations without delay, the estimation of temperature recovered the numerical results across the entire curve.

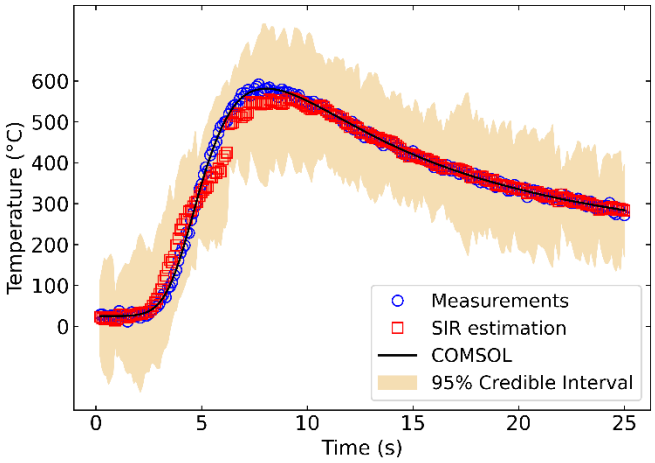

Figure 7. Estimation of measurements of temperature in at $x_1 = 0.02$m with 1000 particles $\sigma_T = 8\% \times Max(T_{Numerical})$ and $\sigma_{\eta_{arc}} = 1\% \times \eta_{arc_0}$.

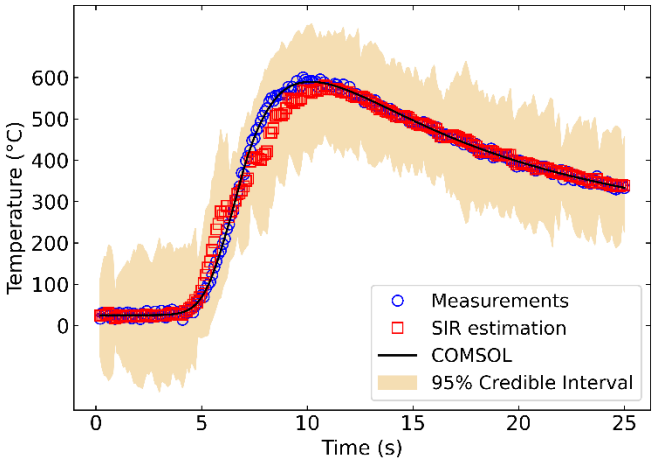

Figure 8. Estimation of measurements of temperature in at $x_2 = 0.03$m with 1000 particles $\sigma_T = 8\% \times Max(T_{Numerical})$ and $\sigma_{\eta_{arc}} = 1\% \times \eta_{arc_0}$.

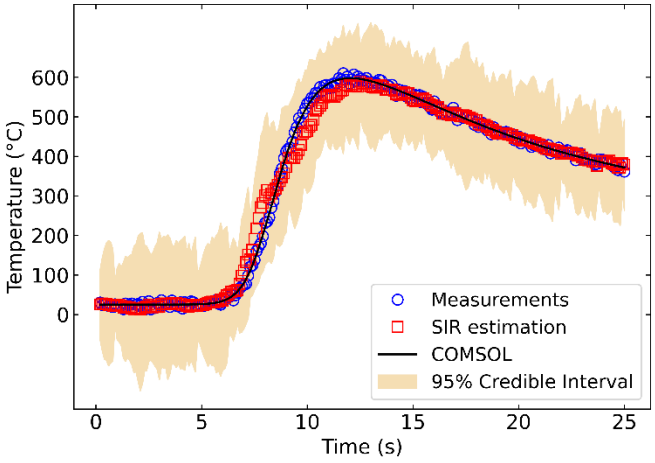

Figure 9. Estimation of measurements of temperature in at $x_3 = 0.04$m with 1000 particles $\sigma_T = 8\% \times Max(T_{Numerical})$ and $\sigma_{\eta_{arc}} = 1\% \times \eta_{arc_0}$.

TABLE IV. RESULTS FOR ARC EFFICIENCY FOR MULTIPLE PARTICLES CONSIDERING $\sigma_{\eta_{arc}} = 1\% \times \eta_0$.

N_{part}	$\sigma_T / Max(T_{Numerical})$	$\mathbf{RMSE}_{\eta_{arc}}$	$\mathbf{Rel}_{\eta_{arc}}$	N_{eff} [%]	Time (s)
100	5%	0.00586856	0.7335703	77.12	27.38
500	5%	0.00345672	0.4320899	79.80	30.27
1,000	5%	0.00063447	0.0793092	81.06	33.79
2500	5%	0.00134992	0.1687402	81.21	42.66
100	8%	0.00390121	0.4876515	75.77	27.25
500	8%	0.00338594	0.4232432	78.88	29.75
1,000	8%	0.00068245	0.0853070	80.65	33.14
2500	8%	0.00166037	0.2075462	78.64	42.11

In addition, the values obtained for the estimation of η_{arc} and for the measured temperatures with 100, 500, 1000 and 2500 particles in the SIR algorithm of the particle filter are presented in Table IV considering $\sigma_{\eta_{arc}} = 1\% \times \eta_{arc_0}$. The results confirm that even considering the direct solution given by Eq. (1) that neglects the temperature dependency of thermal properties, the SIR filter was able to estimate η_{arc} with a relatively small number of particles and reasonable RMSE and Rel, and satisfactory N_{eff}, therefore, no degeneracy of particles occurred. The decrease of RMSE and Rel, as the number of particles increases, indicates more accurate estimations of arc efficiency, but this implies more processing time.

However, it is necessary to determine the minimum number of particles capable of estimating η_{arc}. Considering the process takes place within 25 seconds, the time elapsed in all scenarios is close to the real application time. Nevertheless, with $\sigma_T = 8\% \times Max(T_{Numerical})$, the results suggest that from 1000 particles, there has been no significant improvement in the RMSE and Rel; therefore, the use of 1000 particles would be enough for this estimation.

V. CONCLUSION

This research utilized SIR filter with the direct model of Fachinotti *et al.* [10] to estimate the arc efficiency in a welding process with measures of temperature simulated in COMSOL Multiphysics. The SIR filter was shown to be capable of estimating the arc efficiency, overcoming the limitations of the direct model, when appropriate values of model uncertainty are utilized, within a time interval that is identical to the real process.

ACKNOWLEDGMENT

The authors would like to acknowledge the Province of Nova Scotia for their financial support through the Nova Scotia Graduate Scholarship as well as the Natural Science and Engineering Research Council (NSERC) of Canada for grant support through the Discovery Grant program.

REFERENCES

[1] N. Pépe, S. Egerland, P. A. Colegrove, D. Yapp, A. Leonhartsberger, and A. Scotti, "Measuring the process efficiency of controlled gas metal arc welding processes," Science and Technology of Welding and Joining, vol. 16, pp. 412–417, 2011

[2] J. N. DuPont and A. R. Marder, "Thermal Efficiency of Arc Welding Processes," Welding Journal, vol. 74, pp. 406-416, 1995

[3] M. Mróz, A. W. Orłowicz, M. Lenik, A. Trytek, and M. Tupaj, "Calorimetric Method for the Testing of Thermal Coefficients of the TIG Process," Materials, vol. 15, pp. 7389-7406, 2022.

[4] O. Liskevych, L. Quintino, L. O. Vilarinho, and A. Scotti, "Intrinsic errors on cryogenic calorimetry applied to arc welding," Weld World, vol. 57, pp.349-357, 2013.

[5] E. D. S. Magalhães, A. L. F. D. Lima E Silva, and S. M. M. D. Lima E Silva, "A thermal efficiency analysis of a Gas Tungsten Arch Welding process using a temperature moving sensor," International Journal of Thermal Sciences, vol. 129, pp. 47–55, 2018.

[6] H. R. B. Orlande and M. N. Özişik, Inverse heat transfer: fundamentals and applications, 2nd ed., CRC Press, Taylor & Francis Group, 2021

[7] M. S. Arulampalam, S. Maskell, N. Gordon, and T. Clapp, "A tutorial on particle filters for online nonlinear/non-Gaussian Bayesian tracking," IEEE Trans. Signal Process., vol. 50, pp. 174–188, 2002.

[8] C. V. Gonçalves, L. O. Vilarinho, A. Scotti, and G. Guimarães, "Estimation of heat source and thermal efficiency in GTAW process by using inverse techniques," Journal of Materials Processing Technology, vol. 172, pp. 42–51, 2006.

[9] J. Wang and N. Zabaras, "A Bayesian inference approach to the inverse heat conduction problem," International Journal of Heat and Mass Transfer, vol. 47, pp. 3927–3941, 2004.

[10] V. D. Fachinotti, A. A. Anca, and A. Cardona, "Analytical solutions of the thermal field induced by moving double-ellipsoidal and double-elliptical heat sources in a semi-infinite body," International Journal of Numerical Methods in Biomed Engineering., vol. 27, pp. 595–607, 2011.

[11] J. Goldak, A. Chakravarti, and M. Bibby, "A new finite element model for welding heat sources," MTB, vol. 15, pp. 299–305, 1984.

[12] N. Arruda, J. Carvalho, R. Cruz Neto, D. M. Ferreira, and S. D. Brandi, "Influence of the Heat Flow Transient State on the Microstructure and Microhardness of ASTM-A36 and SAE-1045 Steels Welded by GMAW Process," Soldagem & Inspeção, vol. 24, 15 p., 2019.

[13] J. Kaipio and E. Somersalo, "Statistical and computational inverse problems," Springer e-books, 2005.

[14] B. Ristic, S. Arulampalam, and N. Gordon, Beyond the Kalman filter: particle filters for tracking applications. in Artech House radar library. Boston, MA: Artech House, 2004

[15] Ø. Grong, Metallurgical modelling of welding. Institute of Materials, no. 557. London, 1994

[16] W. B. Da Silva, J. C. S. Dutra, C. E. P. Kopperschimidt, D. Lesnic, and R. G. Aykroyd, "Sequential estimation of the time-dependent heat transfer coefficient using the method of fundamental solutions and particle filters," Inverse Problems in Science and Engineering, vol. 29, pp. 3322–3341, 2021.